TITLE
CHARACTERISATION OF HRAS LOCAL SIGNAL TRANSDUCTION NETWORKS USING ENGINEERED SITE-SPECIFIC EXCHANGE FACTORS

Ana Herrero[a,d], Mariana Reis-Cardoso[a], Iñaki Jiménez-Gómez[b], Carolanne Doherty[a,d], Lorena Agudo-Ibañez[b], Adán Pinto[b], Fernando Calvo[b], Walter Kolch[a,c,d], Piero Crespo[b,e] and David Matallanas[a,d*]

[a] Systems Biology Ireland, University College Dublin, Belfield, Dublin 4, Ireland.

[b] Instituto de Biomedicina y Biotecnología de Cantabria (IBBTEC), Consejo Superior de Investigaciones Científicas (CSIC) - Universidad de Cantabria. Santander 39011, Spain.

[c] Conway Institute, University College Dublin, Dublin 4, Ireland.

[d]School of Medicine and Medical Science, University College Dublin, Belfield, Dublin 4, Ireland

[e] Centro de Investigación Biomédica en Red CIBERONC.

*Corresponding author: david.gomez@ucd.ie orcid.org/0000-0002-2360-3141

WE DECLARE NO CONFLICT OF INTEREST

ABSTRACT

Ras GTPases convey signals from different types of membranes. At these locations, different Ras isoforms, interactors and regulators generate different biochemical signals and biological outputs. The study of Ras localisation-specific signal transduction networks has been hampered by our inability to specifically activate each of these Ras pools. Here, we describe a new set of site-specific tethered exchange factors, engineered by fusing the RasGRF1 CDC25 domain to sub-localisation-defining cues, whereby Ras pools at specific locations can be precisely activated. We show that the CDC25 domain has a high specificity for activating HRas but not NRas and KRas. This unexpected finding means that our constructs mainly activate endogenous HRas. Hence, their use enabled us to identify distinct pathways regulated by HRas in endomembranes and plasma membrane microdomains. Importantly, these new constructs unveil different patterns of HRas activity specified by their subcellular localisation. Overall, the targeted GEFs described herein constitute ideal tools for dissecting spatially-defined HRas biochemical and biological functions.

KEYWORDS

Ras, localisation, Ras-GEF, CDC25 domain, oncogene, signalling network.

Abbreviations:

ER: endoplasmic reticulum
GC: Golgi complex
DM: disordered membrane
LR: Lipid Rafts
GEF: Guanine exchange factor
GAP: GTPase activating protein
PM: Plasma membrane

INTRODUCTION

Ras family small GTPases, including HRas, KRas4A, KRas4B and NRas, function as molecular switches[1]. Mutations in these proteins occur in over 30% of human tumours and Ras oncogenic mutants are some of the main drivers of cancer[2, 3]. Under physiological conditions, Ras cycles between an active state, bound to GTP, and an inactive state, bound to GDP. The Ras activation/deactivation cycle is tightly regulated by two classes of proteins, Guanine Exchange Factors (GEFs), which facilitate Ras activation, and GTPase Activating Proteins (GAPs), which increase Ras GTPase activity, leading to Ras inactivation[2]. Ras proteins regulate a complex signalling network mediated by several effectors including the Raf family kinases, phosphoinositide-3 Kinase (PI3K) and Ral exchange factors. Ras signalling networks ultimately regulate multiple biological responses, including key events such as proliferation, differentiation, migration or survival[2]. Thus, a refined control of the activity of Ras proteins is crucial for eliciting the correct cell fate decisions. Control mechanisms operate at different tiers in order to orchestrate specific Ras-dependent responses, through differential interaction with different effector and regulatory proteins[4]. Another important mechanism for regulating Ras signalling is the localisation-specific control of Ras activation at different membrane domains within the cell, due to the spatially-defined participation of certain exchange factors[5, 6].

Previous studies have unveiled the importance of the site from which Ras signals originate. Initially, it was thought that Ras was functional only at the peripheral plasma membrane, where GEFs would be active[7], but in recent years it has been demonstrated that Ras can also signal from internal localisations such as endoplasmic reticulum (ER)[5], Golgi complex (GC)[8, 9], endosomes[10] or mitochondria[11]. The different Ras isoforms show specific localisation patterns. HRas and NRas signal from the ER and the GC while KRas signalling is mainly

evoked from plasma membrane and mitochondria[12]. Although some Ras interactors are present in all known Ras localisations, a substantial body of data indicates that Ras proteins interact with diverse sets of proteins at distinct sub-localisations, thereby eliciting specific signals from different platforms[12]. Unfortunately, a clear notion of the contribution of the different spatially-defined Ras pools to specific functions is limited by the technical inability to activate the endogenous Ras proteins at, and only at, a specific location. Thus, most of the work done to decipher Ras spatial signalling has been performed by overexpressing tagged constitutively-activated Ras proteins sent to the desired sub-localisations using specific localisation tethers.

In this respect, we have previously reported a comprehensive analysis of HRas site-specific signalling by using the constitutively activated mutant HRas12V, which led us to identify several HRas-dependent functions that are mediated by different spatially-defined HRas pools[8, 13, 14]. However, such an approach has pitfalls, since expression of mutant Ras can have a severe effect in the physiological regulatory mechanism of Ras signalling network which determine Ras activation kinetics in response to physiological signals[15, 16]. This is due to different biochemical properties of HRasV12 which exhibit different affinity and kinetics for Ras interacting proteins compared to wild type HRas[17]. Thus, signals triggered by mut Ras at specific locations may differ from those evoked by wild type (wt) HRas due to their different affinities for GEFs[5, 6, 18] and GAPs[19-21], scaffold proteins[22] and effectors[5, 6, 23, 24]. Importantly, wt Ras is feedback regulated at multiple levels which regulate the duration and intensity of the activation of these GTPases[16]. In particular, the ERK pathway exerts negative feedback to the GEFs and a positive feedback to GAPS, both resulting in downregulation of wt Ras activity. Furthermore there is a positive allosteric feedback from activated Ras to GEFs, such as SOS[25]. All the negative feedbacks are rendered irrelevant by the constitutive activity of mut Ras. However, mut Ras can bind to the allosteric pocket of SOS and stimulate its

activity[25]. Through this positive feedback mut Ras can trigger the aberrant activation of other endogenous Ras isoforms[26], which may confound results when using mut Ras constructs to study Ras site-specific signalling. Therefore, there is an urgent need to develop new methods and strategies in order to characterise local signalling networks activated by Ras under physiological settings.

Here, we present a new set of molecular tools that enable the study of the signalling pathways triggered by endogenous Ras at specific sub-localisations. We demonstrate that these constructs preferentially activate endogenous HRas. Importantly, the signalling networks activated by endogenous HRas reveal similarities but also remarkable differences with those networks evoked by ectopic, site-specific HRasV12 constructs.

RESULTS

Engineering site-specific Ras activator constructs.

In order to study the signals generated by endogenous Ras populations present at their physiological localisations, we engineered a novel set of molecular utensils based on the RasGRF1 CDC25 catalytic domain. It is known that overexpression of an isolated CDC25 domain targeted to the plasma membrane (PM) is sufficient for activating endogenous Ras signalling[27]. Indeed, we ascertained that the expression of CDC25 caused an increase of Ras-GTP levels similar to that elicited by the whole RasGRF1 protein (Fig. 1A). We reasoned that the CDC25 domain specifically targeted to different types of membranes, would be capable of specifically activating the endogenous Ras pools therein, while unaltering physiological regulatory mechanisms acting on Ras signals, such as negative and positive feedbacks or GAPs intervention. To this end, the CDC25 domain was fused to the site-specific tethers previously used to successfully target wild type (wt) HRas and HRasV12 to different cellular compartments[5, 13]. These cues comprised: the avian infectious bronchitis virus M protein

(referred as M1-CDC25 hereafter) to target CDC25 to the endoplasmic reticulum (ER)[28]. For stable expression at the Golgi complex (GC) we used KDEL receptor D193N mutant[6, 29] (KDEL-CDC25). At the PM we analysed two different domains: disordered membrane (DM), using the transmembrane region of the CD8α receptor [30] (CD8-CDC25), and we anchored the CDC25 domain to lipid rafts (LR) using LCK myristoylation signal[31, 32] (LCK-CDC25). A FLAG tag was included to enable the detection of the targeted proteins.

To test that the constructs were correctly expressed and positioned at the desired locations they were transiently transfected in HEK293T cells and their expression was monitored by western blotting (Fig. 1B upper panel). In parallel, we ascertained their localisation by immunofluorescence using anti-FLAG staining and co-localisation with specific localisation markers. The untargeted CDC25 domain was localised throughout the cell apparently associated both with PMs and endomembranes (fig. 1C). Importantly, we observed that the targeted CDC25 proteins specifically localised at the desired localisations with similar expression patterns as those previously described for the HRasV12 constructs [5] (Fig. 1C).

In addition, we generated HeLa cell lines stably expressing the different site–specific GEFs. In these, the expression levels were lower than those obtained by transient expression. In fact, expression was only detectable by previously performing an anti-FLAG immunoprecipitation. (Fig. 1B lower panel).

Altogether, these results indicated that the CDC25 tagged constructs were properly expressed and specifically localised to those compartments where they were aimed at.

Sublocalisation-targeted GEFs specifically activate HRas at different compartments.

Previous studies have shown that RasGRF1 specifically activates HRas, but not NRas and KRas resulting in an activation of ERK1/2[33, 34]. However, it is unclear why RasGRF1 shows such preferences. Structural studies comparing the CDC25 domains of RasGRF1 and SOS1,

suggest that such affinity is not dictated by this domain, requiring the participation of other regulatory motifs present in the GEF [35]. For this reason, we expected our constructs to activate the three Ras isoforms. To confirm this, we analysed the ability of untethered, "global" TOT-CDC25 to activate the three Ras isoforms, by performing Ras-GTP pull down assays in HEK293T cells transiently expressing the GEFs plus wild-type versions of H, K and NRas (Fig. 2A). As expected, EGF treatment activated the three Ras isoforms while RasGRF1 only activated HRas. Surprisingly, we found that TOT-CDC25 prominently activated HRas but not NRas or KRas (Fig 2A upper panel). We also saw that expression of TOT-CDC25 mediated the activation of ERK1/2 and that RasGRF expression and EGF stimulation triggered similar levels of activation of these kinases. Interestingly, only a minimal activation of NRas or KRas could be detected when we doubled the amount of transfected DNA for TOT-CDC25 (Fig. 2A lower panel). This could indicate that the CDC25 domain can also activate these Ras isoforms, though with diminished efficiency. An alternative explanation could be that CDC25-evoked hyperactivation of HRas may promote the activation of the other members of the family, as previously demonstrated[26]. Importantly, this data indicated that the CDC25 domain can contribute to isoform specificity in vivo. This data demonstrated that the CDC25-based constructs are particularly suited for the study of HRas, and therefore we focused on this isoform for the rest of the study.

Next, we investigated the ability of the different site-specific CDC25 constructs to activate the corresponding pools of endogenous HRas. To this end, we utilised the stable HeLa cell lines in which we analysed HRas activation by Ras-GTP pull-down using GST-Raf-RBD. We found that, compared to parental cells, endogenous HRas activation was augmented in all cases, though to different extents. In this cellular context, the ER (M1) and DM (CD8) exhibited the highest levels of Ras activation (Fig. 2B). These results could reflect that, in HeLa cells, HRas is enriched at those sub-localisations where activation is more prominent.

Unfortunately, as of today, there is no reliable methodology to quantitate and compare the levels of endogenous Ras proteins existing at different sub-localisations.

It was important to verify that the tethered-CDC25 constructs activated HRas only at the desired localisation and not unspecifically at other localisations. To test this, the location-specific HRas wild-type versions: M1-HA-HRas (ER-R), LCK-HA-HRas (LR-R), CD8-HA-HRas (DM-R), or KDEL-HA-HRas (GC-R), were co-transfected with the targeted CDC25 proteins. Analysis of their activation in serum-deprived HEK293T cells, confirmed that they were highly GTP-loaded when co-expressed with the CDC25 construct bearing the same tether.

Interestingly, we found that globally-expressed TOT-CDC25 activated endogenous Ras to a lesser extent than the site-specific CDC25 constructs (Fig. 2B), except when targeted to LRs where TOT-CDC25 induce similar level of activation of LR-R than LCK-CDC25 (Fig. 2C). Importantly, we saw that TOT-CDC25 and LCK-CDC25 induce similar levels of activation of endogenous HRas (fig. 2B). Taking together both observations the data would suggest that untargeted CDC25 mainly activates HRas at this sublocalisation.

Noticeably, some unspecific activation was apparent, especially in the case of PM microdomains (Fig. 2C). This could be due to the cross-activation of HRas pools located at the boundaries of DM and LR microdomains. In addition, vesicle trafficking between endomembranes and the peripheral PM may also contribute to some unspecific activation of HRas by reshuffling the localisation of the CDC25 constructs.

In summary, these experiments strongly indicated that the location-specific CDC25 constructs mainly activate the HRas pool located at the specific sublocalisation where these proteins are expressed.

Ras effectors are differentially regulated depending on the subcellular localisation where endogenous Ras is activated.

Next, we tested whether the activation of endogenous HRas at different subcellular compartments could differentially activate known Ras effector pathways. Our previous studies of KRas-dependent regulation of RASSF1A/MST2 demonstrated the importance of the differences in the activation kinetics of oncogenic vs wild-type Ras in the regulation of cell death and proliferation[17, 36]. This study also demonstrated that the dynamics and magnitude of Ras signalling network could be cell type specific. Therefore, we compared effector usage in response to endogenous, site-specific HRas activation, as evoked by the tethered CDC25 constructs, to that elicited by the presence of ectopic HRasV12 at the same sites. We performed these experiments in NIH 3T3 cells, previously used to characterise effector pathway activation by tethered HRasV12 constructs[13]. We found that both sets of constructs elicited a similar pattern of ERK1/2 activation (Fig. 3A). Interestingly, in the case of ER-emanating signals (M1), endogenous HRas was more efficient than its oncogenic version for triggering ERK activation. Overall, notwithstanding expected differences in intensities, endogenous Ras activation, as evoked by site-specific GEFs, and site-restricted HRasV12 oncoproteins elicited similar patterns of ERK activation.

We extended our analyses to other well-characterised Ras effectors, by monitoring the changes on AKT phosphorylation, one of the key components of the PI3K cascade. The phosphorylation status of AKT exhibited remarkable differences when elicited by endogenous HRas activated by the targeted GEFs at different locations. Interestingly, the two phosphorylatable residues needed for full activation of the kinase[37-39], threonine 308 (T308) and serine 473 (S473), exhibited distinct phosphorylation patterns depending on the sub-localisation where HRas was activated (Fig. 3B). While PDK1-dependent T308 phosphorylation[40] was mainly evoked from LR, where PDK1 is located[41], S473

phosphorylation mainly resulted as a consequence of HRas signals coming from DM and endomembranes but not from LR (Fig. 3B upper panel). Since AKT-S473 is phosphorylated by mTORC2 [38], our results are in line with previous reports indicating that AKT-T308 and S473 residues may be phosphorylated in different cell compartments due to differential localisation of PDK1 and mTORC2 [42, 43]. In the case of mTORC2, which localises to endomembranes, and possibly at some specific PM domains, it suggests that this kinase could be activated by HRas-induced mechanisms at these locations. Thus, these results shed light on the relevance of mTORC2 localisation at the PM, hitherto not well characterised. It has been proposed that mTORC2 is recruited to LR by AKT and that this complex may translocate to DM upon activation to allow its dephosphorylation[42, 43]. Our results would confirm that mTORC2 is differentially activated at PM microdomains, but contrary to previous reports, they strongly indicate that the activation of mTORC2 induced by HRas [44] occurs at the DM.

The suitability of the site-specific GEFs for deciphering localised HRas signalling, was further confirmed when we studied the activation of the stress activated kinase JNK1. We observed that JNK was differentially regulated, to some extent, from all locations. Although the site-related differences on JNK activation are small, we consistently observed that activation from GC significantly evoked higher levels of phosphorylated JNK (Fig. 3B middle) while JNK activity as regulated from the ER and DM was less potent. In addition, we analysed STAT3 phosphorylation (Y705) after local HRas activation. This phosphorylation has been reported to be responsible for its dimerisation, translocation to the nucleus and DNA binding, which is essential for STAT3-dependent regulation of cell cycle and survival genes[45-47]. We found that site-specific GEFs induced STAT3 phosphorylation from all locations but preferentially from the GC (Fig. 3B lower panel).

The above results confirmed that endogenous HRas activates different signalling pathways at distinct cellular localisation. Importantly, these results showed some differences on the pattern of activation of HRas signalling pathways compared to what we observed in our previous studies using constructs expressing site-specific HRasV12[13]. The fact that we did not find the same pattern of effector activation suggests that wild-type and oncogenic HRas are not equivalent in their regulation of effector networks. Altogether, our data demonstrate that our site-specific GEFs can be useful tools for the study of HRas signalling variability as orchestrated by space.

Regulation of proliferation and survival by Ras activity induced by site-specific GEFs.

We next used the CDC25 targeted constructs to investigate the contribution of the different subcellular pools of endogenous HRas to several biological outcomes. Our previous studies using NIH 3T3 stable cell lines expressing targeted HRasV12 proteins, demonstrated that proliferation was differentially regulated depending on localisation[13]. For this reason, we analysed if activation of endogenous HRas by the site-specific GEFs followed the same pattern. We found that Ras signalling from PM microdomains (LR and DM) had the highest impact on proliferation (Fig. 4A). This result was identical to that we had previously observed when using targeted HRasV12[13]. It confirmed that constant HRas activation from the PM evokes a proliferative advantage, regardless whether the HRas activation is caused by mutation or chronic GEF stimulation.

Next, we examined cell survival using two different assays. First, we measured the bulk survival rates of confluent cells expressing the different targeted GEFs constructs under conditions of serum depravation (Fig. 4B). In this case, we did not observe significant differences. However, when we measured clonal survival by colony formation assays, where cells are evaluated for their capacity to survive and form colonies originating from single

cells, our data showed that CDC25-induced chronic activation of HRas provided pro-survival signals from LR, DM and GC but not from the ER (Fig. 4C). Significantly, this result is very different from our previous observations using the oncogenic HRasV12 constructs, where we saw a clear pro-survival advantage emanating from the ER and no regulation from the GC[13]. This difference suggested the existence at the ER of some down-regulatory mechanism for HRas signals that modulates this biological function. Interestingly, the results might indicate that oncogenic HRasV12 is insensitive to such regulation, triggering pro-survival signals from the ER that may contribute to HRasV12-dependent transformation. Distinguishing between these possibilities will require the identification of the regulatory mechanism in future studies.

The site-specific CDC25 have limited transforming potential.

Constitutively active HRasV12 is a driver of cell transformation[1], primarily due to aberrant regulation of the activation status of its effector pathways[48]. Expression of the site-specific HRasV12 constructs induced similar levels of transformation than HRasV12 in NIH 3T3 cells with the exception of HRasV12 localised to the GC. It has also been reported that expression of full length RasGRF1 and PM targeted CDC25 domain transform NIH 3T3 cell due to the hyperactivation of HRas signalling[27, 49]. For this reason, we next examined whether our site-specific CDC25 differentially mediated transformation. To this end, we performed focus formation assays in NIH 3T3 fibroblasts using the *bona fide* oncogene HRasV12 as positive control[1]. As expected HRasV12 induced the formation of transformed foci in less than 2 weeks. Similar to previous studies demonstrating that the expression of an isolated CDC25 domain does not induce transformation in NIH 3T3 cells[27], our results clearly showed that overexpression of the TOT-CDC25 did not result in cellular transformation (Fig. 5). Interestingly, expression of the site-specific CDC25 constructs had very limited

transforming effect and only after three weeks in culture we could observe the formation of some transformed foci. We observed that CDC25 expression in the endomembranes induced lower number of transformed foci and they were similar in shape to the spontaneous foci observed in the control cells indicating that activation of endogenous Ras at these locations does not mediate cell transformation. In the case of the constructs targeted to the PM we observed the formation of some transformed foci that resemblance HRasV12-induced foci and LR-CDC25 induced more transformed foci (27 foci/μg DNA) than DM-CDC25 (20 foci/μg DNA). Remarkably, our results are consistent with previous results from Der's group using CAAX-CDC25, which also targets CDC25 to the PM, and showed similar transforming potential (23 foci/μg DNA) to LCK- and CD8-CDC25[27].

Hence, our findings showed that the targeted CDC25-GEF domains can induce activation of endogenous HRas but, unlike hyperactive HRasV12, this results in very limited cellular transformation.

Discussion.

Our understanding of the functional differences among Ras isoforms has increased since seminal studies by Mark Phillips and John Hancock demonstrated that Ras proteins are active in endomembranes and in different PM microdomains [50, 51], where they have different sets of interactors. Unfortunately, despite the growing importance of space as a regulator of Ras signalling, we still lack the technology to specifically and physiologically activate compartmentalised pools of Ras. For this reason we must rely on the use of different molecular tools to decipher Ras spatial regulation. Therefore, the CDC25-based site-specific constructs described herein are valuable tools for this purpose. These constructs are an important addition to the series of molecular utensils that we and others have developed in the past, to understand the role of the different cellular pools of Ras in the diverse plethora of

biological outcomes regulated by these proteins[5, 11, 13, 15]. Unexpectedly, we found that the CDC25 domain exhibits a strong specificity for HRas, and only when expressed at high levels we could detect modest activation of NRas and KRas.

A comparison of the biochemical effects caused by the expression of the site-specific CDC25 and HRasV12 constructs demonstrate that there are differences in the signals induced by both set of tools. Thus, while we do not observe major differences in the pattern of activation of ERK from the different locations, there were clear differences in AKT phosphorylation patterns. We previously showed that the phosphorylation of AKT at S473 was induced to similar levels by the expression of site-specific HRasV12 constructs with the exception of HRasV12 localised to the GC[13]. Remarkably, the expression of CDC25 at the GC caused a clear induction of AKT phosphorylation at S473, while no phosphorylation was induced by CDC25 localised in LR. Similarly, the activation of JNK induced by the expression of the CDC25 constructs is weaker than that elicited by site-specific HRasV12 constructs. We also observe a different pattern of JNK activation: only CDC25 expressed in the GC activates JNK, whereas HRasV12 induced the strongest JNK activation when targeted to the DM.[13]

The differences in the activation of HRas effectors by these two sets of tools is likely responsible for differences of the biological phenotypes induced by these constructs. We demonstrate that the site-specific CDC25 constructs triggered differential HRas-dependent functions as summarised in Figure 6. These results are most readily explained by the differential abundance and regulation of specific HRas regulators and effectors at a given location, as illustrated by the differential regulation of the two key phosphorylation residues of AKT. Importantly, although both sets of constructs activate the HRas signalling network and have many similar biochemical and biological effects, there were also exceptions. Interestingly, the targeted CDC25 and HRasV12 constructs differ in their effects on cell transformation, which may indicate that transformation depends more closely on the exact

intensity and dynamics of HRas signalling than other biological effects. Only the PM-targeted CDC25 constructs induced the formation of some transformed foci of NIH 3T3 cells that were similar to Ras-induced foci and only after three weeks we could observe some macroscopic transformed foci; while HRasV12 targeted to different locations induced similar levels of transformation than untargeted HRasV12 with the important exception of HRasV12 targeted to the GC[13]. These differences could be explained by two scenarios. One possibility is that even though the site-specific GEFs can constantly activate HRas and induce proliferative and survival advantages, their effect on local HRas pools is not strong enough to induce cellular transformation. A second, and not mutually exclusive possibility, is that HRas-mediated signals, as induced by site-specific GEFs, remain under the control of negative or positive feedback loops and cross-talks with other signalling pathways that preclude transformation. For instance, unlike CDC25-activated endogenous HRas, mut HRas is no longer sensitive to the regulatory effect of the ERK-RSK1/2-NF1 positive feedback loop, which ultimately results in different ERK activation dynamics and would explain the different phenotype[52]. Additionally, structural changes on mutant HRas could result in the establishment of aberrant protein-protein interactions[53], which may lead to the development of pathological feedback loops or cross-talks with other signalling pathways.

Another clear difference that we have observed is that, unlike M1-HRasV12, activation of endogenous HRas in the ER by M1-CDC25 is not sufficient to activate a pro-survival signal. Notwithstanding other possible mechanisms, a simple explanation for this observation could be the existence of a specific HRas GAP at the ER that inactivates wt HRas while the GAP-insensitive HRasV12 evokes the constant activation in this localisation of effectors responsible for the pro-survival signal[54]. The existence of site-specific interactors and/or effectors is likely responsible for the surprising observation that HRas localised to the PM

domains induce a higher proliferation rate than HRas located in the ER, despite this is the localisation where ERK and AKT activation is stronger.

In summary, our results indicate that site-specific CDC25 constructs are appropriate tools for the study of spatially-defined HRas signalling and that they generate a response closer to physiology than that one obtained by the use of homologous HRasV12 constructs, utilised in previous studies. Finally, these results indicate that the combination of these tools in comparative studies can be used to gain insights into the regulatory mechanisms orchestrating spatially defined Ras signals, and will be helpful for deciphering the spatial cues regulating oncogenic Ras transforming properties. These studies will help in completing our understanding of Ras-dependent signalling networks that have not been fully characterised despite intensive work in the last three decades[55].

METHODS

Constructs

pGEX-Raf-RBD, HA-RasGRF1, pCEFL-FLAG-RasV12 and the RasV12 plasmids targeted to be expressed at different compartments were previously used and described[5, 13, 34]. CDC25 domain from the RasGRF1 plasmid described before[49] (only RasGEF motif containing codons 947-1273) was amplified by PCR and cloned into pCEFL-FLAG vector, sequences of the oligonucleotides utilised are available upon request. The same epitopes and localisation signals used for pCEFL-FLAG-HRasV12 [13] were used for the generation of M1-FLAG-CDC25, LCK-FLAG-CDC25, CD8-FLAG-CDC25 and KDEL-FLAG-CDC25 by cloning the newly generated FLAG-CDC25 in the C-terminal of the different localisation-targeting vectors. All sequences were verified by DNA sequencing.

Cell culture

HEK293T, NIH 3T3, HeLa and COS-1 cells were grown in Dulbecco modified Eagle medium (DMEM) supplemented with 10% FBS (foetal bovine serum) and L-glutamine (2 mM) at 37 ºC and 5% CO_2. Cells were transfected with Lipofectamine 2000 (Invitrogen) according with manufacturer's instruction and the amount of DNA indicated in each experiment. For the generation of HeLa stable cell lines, the targeted CDC25 plasmids were transfected in HeLa cells and selection of clones expressing the different CDC25 was performed by G418 (750 μg/ml) treatment during 2 weeks.

Cell lysis and immunoblotting

Total cellular extracts were obtained after cell lysis with HEPES pH 7.5 20 mM, NaCl 150 mM, 1% NP-40 and proteases and phosphatases inhibitors. Total lysates were analysed by SDS-polyacrylamide gel electrophoresis and transferred to PVDF membranes. The following antibodies were used: HA (sc-7392) and total AKT1 (sc-5298) from Santa Cruz; FLAG-M2 (A8592 mouse), FLAG (7425 rabbit), phospho-ERK1/2 (M8159) and total ERK1/2 (M5670) from Sigma; pan-Ras (op40) from Calbiochem; α1 Sodium potassium APTase (AB7671) from Abcam; GM130 (610822) from BD; Calnexin (2679); phospho-AKT T308 (9275), phospho-AKT S473 (9271), phospho-JNK (9251), total JNK1 (9252), phospho-STAT3 (9131), total STAT3 (9132) and GADPH (2118) from Cell Signalling, secondary mouse (7076) and rabbit (7074) peroxidase-conjugated antibodies from Cell Signalling. EGF was from Upstate Biotechnology Inc.

Immunofluorescence

COS-1 cells were plated and transfected with TransIT-X2 (Mirus) following manufacturer's instruction. Cells were fixed and immunostained as previously described[13]. Briefly, cells were fixed with 3.7% formaldehyde in BS for 10min. Subsequently the fixed cell were permiabilised with 0.5% Triton X-100-PBS (15 min), followed by 0.1 M glycine-PBS (30min). After blocking with 1% BSA-0.01% Tween 20 in PBS (5 min) the cells were

incubated with the primary antibodies for an hour. GM130 (mouse), Na/K ATPase (mouse), Calnexin (Rabbit) specific antibodies and Cholera Toxin Subunit B (Recombinant) Alexa Fluor™ 488 Conjugate C34775 (ThermoFisher), that recognises ganglioside GM1 were used for the detection of endogenous markers. FLAG-M2 (mouse) was used to stain M1-CDC25 and FLAG antibody (Rabbit) for the rest of the tagged proteins. Next the cells were washed and incubated with Alexa secondary antibodies conjugated to fluorophores for 45 min. VECTASHIELD anti-fade mounting media with DAPI (Vector Laboratories) was used to mount the slides. The localisation was determined by confocal microscopy (Leica TCS SP5) at excitation wavelengths of 488 nm (green) and 594 nm (red).

Ras activity assays

Ras activity assays were performed by Raf-RBD pull-down as previously described[13]. Briefly, cells were lysed using magnesium rich lysis bugger (25 mM HEPES, pH 7.5, 10 mM MgCl2, 150 mM NaCl, 0.5 mM EGTA, 20 mM β-glycerophosphate, 0.5% Nonidet-P40, 10% glycerol, 2 mM sodium orthovanadate, 25 μg/ml leupeptin, and 25 μg/ml aprotinin). Cell lyses were incubated rotating for 1 hour at 4ºC with glutathione agarose beads conjugated with GST-RBD, which contains Raf's Ras binding domain. Ras-GTP bound to the GST-RBD beads was pulled-down by short centrifugations. The beads were washed three times using lysis buffer without glycerol. Laemmli buffer was added to the dry beads and the proteins were denaturalised by boiling the samples which were next analysed by western blot. Ras-GTP fraction was detected with pan-Ras antibody for the endogenous Ras or HA antibody for the transfected Ras isoforms. Ras-GTP levels were normalised against determined total levels of Ras in the corresponding total lysates.

Proliferation assays

Proliferation analysis was performed as previously described[13]. Briefly, NIH 3T3 cells were plated at a density of 50,000 cells per well in a six-well plate in duplicates and grown in 5%

FBS containing media. Every 24 hours, cells were detached and resuspended using 0.5 ml of trypsin and counted using the Countess Automated Cell Counter (Life Technologies) following manufacturer's instructions.

Survival curves

To estimate survival rates NIH 3T3 cells were plated at high density in a six-well plate in duplicates and grown in 1% FBS containing media. Cells were counted every 24 hours for 3 days by standard cell counting techniques as indicated above.

G418-resistant colonies formation

Colony formation assays were performed as described previously in Matallanas et al.[13] NIH 3T3 cells were plated at low confluence and transfected with 0.5 μg of the indicated plasmids. Cells were grown in DMEM supplemented with 10% calf serum in the presence of G418 (750 μg/ml) for 10-15 days to allow the formation of discrete colonies. For scoring, cells were fixed, stained with GIEMSA, and colonies with a diameter bigger than 1 mm were counted.

Transformation assays

Focus formation assay was performed as established by Aaronson et al [56]. Briefly, 30% confluent NIH 3T3 were plated and transfected using Lipofectamine with low amounts of the indicated plasmids and grown for 3 weeks in DMEM supplemented with 10% calf serum. The media was changed every 3 days and transformation of cells and the formation of foci was monitored using microscopy and visual inspection. When the focus were macroscopically detected by eye the cells were fixed and stained, and foci scored.

FUNDING

This work was supported by the Science Foundation Ireland under grant no. 06/CE/B1129 (AH, CD, DM and WK) and grant no. 15/CDA/3495 (DM, MRC); and PC lab is supported by grant BFU2011-23807 from the Spanish Ministry of Economy–Fondos FEDER; and by the Red Temática de Investigación Cooperativa en Cáncer (RTICC) (RD/12/0036/0033);and Spanish Ministry of Health; and by Asociación Española Contra el Cáncer (AECC), grant GCB141423113.

References

1. Barbacid M. ras genes. Annu Rev Biochem 1987; 56:779-827.
2. Downward J. Targeting RAS signalling pathways in cancer therapy. Nat Rev Cancer 2003; 3:11-22.
3. Karnoub AE, Weinberg RA. Ras oncogenes: split personalities. Nat Rev Mol Cell Biol 2008; 9:517-31.
4. Calvo F, Agudo-Ibanez L, Crespo P. The Ras-ERK pathway: understanding site-specific signaling provides hope of new anti-tumor therapies. Bioessays 2010; 32:412-21.
5. Arozarena I, Matallanas D, Berciano MT, Sanz-Moreno V, Calvo F, Munoz MT, et al. Activation of H-Ras in the endoplasmic reticulum by the RasGRF family guanine nucleotide exchange factors. Molecular and cellular biology 2004; 24:1516-30.
6. Caloca MJ, Zugaza JL, Bustelo XR. Exchange factors of the RasGRP family mediate Ras activation in the Golgi. J Biol Chem 2003; 278:33465-73.
7. Quilliam LA, Khosravi-Far R, Huff SY, Der CJ. Guanine nucleotide exchange factors: activators of the Ras superfamily of proteins. Bioessays 1995; 17:395-404.
8. Chiu VK, Bivona T, Hach A, Sajous JB, Silletti J, Wiener H, et al. Ras signalling on the endoplasmic reticulum and the Golgi. Nature cell biology 2002; 4:343-50.
9. Choy E, Chiu VK, Silletti J, Feoktistov M, Morimoto T, Michaelson D, et al. Endomembrane trafficking of ras: the CAAX motif targets proteins to the ER and Golgi. Cell 1999; 98:69-80.
10. Lu A, Tebar F, Alvarez-Moya B, Lopez-Alcala C, Calvo M, Enrich C, et al. A clathrin-dependent pathway leads to KRas signaling on late endosomes en route to lysosomes. J Cell Biol 2009; 184:863-79.
11. Bivona TG, Quatela SE, Bodemann BO, Ahearn IM, Soskis MJ, Mor A, et al. PKC regulates a farnesyl-electrostatic switch on K-Ras that promotes its association with Bcl-XL on mitochondria and induces apoptosis. Molecular cell 2006; 21:481-93.

12. Arozarena I, Calvo F, Crespo P. Ras, an actor on many stages: posttranslational modifications, localization, and site-specified events. Genes & cancer 2011; 2:182-94.
13. Matallanas D, Sanz-Moreno V, Arozarena I, Calvo F, Agudo-Ibanez L, Santos E, et al. Distinct utilization of effectors and biological outcomes resulting from site-specific Ras activation: Ras functions in lipid rafts and Golgi complex are dispensable for proliferation and transformation. Molecular and cellular biology 2006; 26:100-16.
14. Agudo-Ibanez L, Nunez F, Calvo F, Berenjeno IM, Bustelo XR, Crespo P. Transcriptomal profiling of site-specific Ras signals. Cell Signal 2007; 19:2264-76.
15. Aran V, Prior IA. Compartmentalized Ras signaling differentially contributes to phenotypic outputs. Cell Signal 2013; 25:1748-53.
16. Fey D, Matallanas D, Rauch J, Rukhlenko OS, Kholodenko BN. The complexities and versatility of the RAS-to-ERK signalling system in normal and cancer cells. Semin Cell Dev Biol 2016; 58:96-107.
17. Matallanas D, Romano D, Al-Mulla F, O'Neill E, Al-Ali W, Crespo P, et al. Mutant K-Ras activation of the proapoptotic MST2 pathway is antagonized by wild-type K-Ras. Mol Cell 2011; 44:893-906.
18. Roose JP, Mollenauer M, Ho M, Kurosaki T, Weiss A. Unusual interplay of two types of Ras activators, RasGRP and SOS, establishes sensitive and robust Ras activation in lymphocytes. Molecular and cellular biology 2007; 27:2732-45.
19. Cozier GE, Lockyer PJ, Reynolds JS, Kupzig S, Bottomley JR, Millard TH, et al. GAP1IP4BP contains a novel group I pleckstrin homology domain that directs constitutive plasma membrane association. J Biol Chem 2000; 275:28261-8.
20. Li C, Cheng Y, Gutmann DA, Mangoura D. Differential localization of the neurofibromatosis 1 (NF1) gene product, neurofibromin, with the F-actin or microtubule cytoskeleton during differentiation of telencephalic neurons. Brain Res Dev Brain Res 2001; 130:231-48.
21. Nordlund M, Gu X, Shipley MT, Ratner N. Neurofibromin is enriched in the endoplasmic reticulum of CNS neurons. J Neurosci 1993; 13:1588-600.
22. Casar B, Arozarena I, Sanz-Moreno V, Pinto A, Agudo-Ibanez L, Marais R, et al. Ras subcellular localization defines extracellular signal-regulated kinase 1 and 2 substrate specificity through distinct utilization of scaffold proteins. Molecular and cellular biology 2009; 29:1338-53.
23. Morice C, Nothias F, Konig S, Vernier P, Baccarini M, Vincent JD, et al. Raf-1 and B-Raf proteins have similar regional distributions but differential subcellular localization in adult rat brain. Eur J Neurosci 1999; 11:1995-2006.
24. Yuryev A, Ono M, Goff SA, Macaluso F, Wennogle LP. Isoform-specific localization of A-RAF in mitochondria. Molecular and cellular biology 2000; 20:4870-8.
25. Boykevisch S, Zhao C, Sondermann H, Philippidou P, Halegoua S, Kuriyan J, et al. Regulation of ras signaling dynamics by Sos-mediated positive feedback. Curr Biol 2006; 16:2173-9.
26. Jeng HH, Taylor LJ, Bar-Sagi D. Sos-mediated cross-activation of wild-type Ras by oncogenic Ras is essential for tumorigenesis. Nat Commun 2012; 3:1168.
27. Quilliam LA, Huff SY, Rabun KM, Wei W, Park W, Broek D, et al. Membrane-targeting potentiates guanine nucleotide exchange factor CDC25 and SOS1 activation of Ras transforming activity. Proceedings of the National Academy of Sciences of the United States of America 1994; 91:8512-6.
28. Swift AM, Machamer CE. A Golgi retention signal in a membrane-spanning domain of coronavirus E1 protein. J Cell Biol 1991; 115:19-30.

29. Cole NB, Smith CL, Sciaky N, Terasaki M, Edidin M, Lippincott-Schwartz J. Diffusional mobility of Golgi proteins in membranes of living cells. Science 1996; 273:797-801.
30. Arcaro A, Gregoire C, Boucheron N, Stotz S, Palmer E, Malissen B, et al. Essential role of CD8 palmitoylation in CD8 coreceptor function. J Immunol 2000; 165:2068-76.
31. Resh MD. Membrane targeting of lipid modified signal transduction proteins. Subcell Biochem 2004; 37:217-32.
32. Su MW, Yu CL, Burakoff SJ, Jin YJ. Targeting Src homology 2 domain-containing tyrosine phosphatase (SHP-1) into lipid rafts inhibits CD3-induced T cell activation. J Immunol 2001; 166:3975-82.
33. Jones MK, Jackson JH. Ras-GRF activates Ha-Ras, but not N-Ras or K-Ras 4B, protein in vivo. J Biol Chem 1998; 273:1782-7.
34. Matallanas D, Arozarena I, Berciano MT, Aaronson DS, Pellicer A, Lafarga M, et al. Differences on the inhibitory specificities of H-Ras, K-Ras, and N-Ras (N17) dominant negative mutants are related to their membrane microlocalization. J Biol Chem 2003; 278:4572-81.
35. Freedman TS, Sondermann H, Kuchment O, Friedland GD, Kortemme T, Kuriyan J. Differences in flexibility underlie functional differences in the Ras activators son of sevenless and Ras guanine nucleotide releasing factor 1. Structure 2009; 17:41-53.
36. Romano D, Maccario H, Doherty C, Quinn NP, Kolch W, Matallanas D. The differential effects of wild-type and mutated K-Ras on MST2 signaling are determined by K-Ras activation kinetics. Mol Cell Biol 2013; 33:1859-68.
37. Bozulic L, Hemmings BA. PIKKing on PKB: regulation of PKB activity by phosphorylation. Curr Opin Cell Biol 2009; 21:256-61.
38. Sarbassov DD, Guertin DA, Ali SM, Sabatini DM. Phosphorylation and regulation of Akt/PKB by the rictor-mTOR complex. Science 2005; 307:1098-101.
39. Alessi DR, Andjelkovic M, Caudwell B, Cron P, Morrice N, Cohen P, et al. Mechanism of activation of protein kinase B by insulin and IGF-1. EMBO J 1996; 15:6541-51.
40. Alessi DR, James SR, Downes CP, Holmes AB, Gaffney PR, Reese CB, et al. Characterization of a 3-phosphoinositide-dependent protein kinase which phosphorylates and activates protein kinase Balpha. Curr Biol 1997; 7:261-9.
41. Reis-Sobreiro M, Roue G, Moros A, Gajate C, de la Iglesia-Vicente J, Colomer D, et al. Lipid raft-mediated Akt signaling as a therapeutic target in mantle cell lymphoma. Blood Cancer J 2013; 3:e118.
42. Betz C, Hall MN. Where is mTOR and what is it doing there? J Cell Biol 2013; 203:563-74.
43. Hill MM, Feng J, Hemmings BA. Identification of a plasma membrane Raft-associated PKB Ser473 kinase activity that is distinct from ILK and PDK1. Curr Biol 2002; 12:1251-5.
44. Boulbes D, Chen CH, Shaikenov T, Agarwal NK, Peterson TR, Addona TA, et al. Rictor phosphorylation on the Thr-1135 site does not require mammalian target of rapamycin complex 2. Mol Cancer Res 2010; 8:896-906.
45. Shirogane T, Fukada T, Muller JM, Shima DT, Hibi M, Hirano T. Synergistic roles for Pim-1 and c-Myc in STAT3-mediated cell cycle progression and antiapoptosis. Immunity 1999; 11:709-19.
46. Barre B, Vigneron A, Coqueret O. The STAT3 transcription factor is a target for the Myc and riboblastoma proteins on the Cdc25A promoter. J Biol Chem 2005; 280:15673-81.

47. Sellier H, Rebillard A, Guette C, Barre B, Coqueret O. How should we define STAT3 as an oncogene and as a potential target for therapy? JAKSTAT 2013; 2:e24716.
48. Bos JL. ras oncogenes in human cancer: a review. Cancer research 1989; 49:4682-9.
49. Arozarena I, Aaronson DS, Matallanas D, Sanz V, Ajenjo N, Tenbaum SP, et al. The Rho family GTPase Cdc42 regulates the activation of Ras/MAP kinase by the exchange factor Ras-GRF. J Biol Chem 2000; 275:26441-8.
50. Prior IA, Harding A, Yan J, Sluimer J, Parton RG, Hancock JF. GTP-dependent segregation of H-ras from lipid rafts is required for biological activity. Nature cell biology 2001; 3:368-75.
51. Fehrenbacher N, Bar-Sagi D, Philips M. Ras/MAPK signaling from endomembranes. Mol Oncol 2009; 3:297-307.
52. Hennig A, Markwart R, Wolff K, Schubert K, Cui Y, Prior IA, et al. Feedback activation of neurofibromin terminates growth factor-induced Ras activation. Cell Commun Signal 2016; 14:5.
53. Engin HB, Carlin D, Pratt D, Carter H. Modeling of RAS complexes supports roles in cancer for less studied partners. BMC Biophys 2017; 10:5.
54. Maertens O, Cichowski K. An expanding role for RAS GTPase activating proteins (RAS GAPs) in cancer. Adv Biol Regul 2014; 55:1-14.
55. Stephen AG, Esposito D, Bagni RK, McCormick F. Dragging ras back in the ring. Cancer Cell 2014; 25:272-81.
56. Aaronson SA, Todaro GJ, Freeman AE. Human sarcoma cells in culture. Identification by colony-forming ability on monolayers of normal cells. Exp Cell Res 1970; 61:1-5.

FIGURE LEGENDS

Figure 1. Validation of the constructs for the expression of CDC25 at different compartments within the cell. A. *Expression of RasGRF1 CDC25 domain activates Ras.* HEK293T cells were transfected with 0.5 μg of HA-RasGRF1 or FLAG-CDC25 or stimulated with EGF (100 ng/ml) for 5 minutes. Cells were serum deprived for 16h. Cell lysates were incubated with GST-Raf-RBD and the activation of endogenous Ras was determined by pull-down assays. Activation of Ras and ERK was monitored using the indicated antibodies. The figure is representative of 3 independent experiments. B. *Expression of targeted CDC25 domain at different sub-localisations*. HEK293T cells were transiently transfected with 0.5 μg of DNA with FLAG-CDC25 (TOT), M1-FLAG-CDC25 (ER), LCK-FLAG-CDC25 (LR), CD8-FLAG-CDC25 (DM) and KDEL-FLAG-CDC25 (GC). Protein expression was tested by anti-FLAG immunoblotting in total lysates from the transiently transfected HEK293T cells (upper) and from FLAG immunoprecipitates from the stable HeLa cell lines (lower). C. *Cellular sub-localisation of targeted CDC25 domain*. COS-1 cells were co-transfected with 0.5 μg of each CDC25 plasmid as indicated. Fixed cells were stained with anti-FLAG antibody to detect CDC25 constructs (red) and co-immunostained with markers of subcellular membranes (green): Calnexin (ER); Alexa 488-cholera toxin that stains GM1 (LR); Na/K ATPase (DM); and GM130 (GC). Nuclei were stained with DAPI (blue). Co-localisation was analysed by confocal imaging.

Figure 2. The CDC25 domain is able to activate HRas at different subcellular compartments. A. *Ras activation by CDC25 domain expression is isoform specific*. (*Upper panel)* HEK293T cell were co-transfected with 0.5 μg HA-HRas, HA-KRas, HA-NRas, HA-

RasGRF1(0.5 μg), FLAG-CDC25 (0.5 μg) or treated with EGF (100 ng/ml) for 5 min as indicated; *(Lower panel*) HEK293T cells were transfected with mock DNA (-) or co-transfected with 0.5 μg of HA-HRas wt, HA-NRas wt or HA-KRas wt and 1 μg of FLAG-CDC25 or 1 μg of mock DNA as indicated. 24 hours after transfection the cells were serum deprived (16 hours), and Ras activation was analysed by pull-down assays using the GST-Raf-RBD recombinant protein. Activation of the different isoforms was measured by Western-blot with anti-HA antibody in the pulled-down fraction and in the total lysates. The data shows HA-Ras-GTP levels normalised to the total HA-Ras, and represented as fold induction relative to the Ras-GTP levels in control cells (in absence of FLAG-CDC25) for each isoform. The data shows the average of two independent experiments and error bars represent standard deviation (SD). Anti-FLAG blot upper panel was spliced from the same gel. B. *Activation of endogenous Ras by targeted CDC25 domain at different sub-localisation*. HeLa stable cell lines expressing CDC25 at different subcellular compartments were lysed 16 hours after serum starvation. Total lysates were incubated with GST-Raf-RBD recombinant protein for pulling-down active Ras (Ras-GTP). Total Ras levels were determined by immunoblotting. Ras activation was normalised against the total Ras, and is represented as fold induction relative to the Ras-GTP levels in control cells (ST). The data shows the average ± the SD of two independent experiments. C. *Targeted CDC25 domain specifically activates Ras at each subcellular site*. Activated Ras at different compartments was analysed using pulldown assays with GST-Raf-RBD recombinant protein and further anti-Ras immunoblotting. HEK293T cells were transfected with 0.5 μg of M1-HA-HRas wt, LCK-HA-HRas wt, CD8-HA-HRas wt, or KDEL-HA-HRas wt, in addition to 0.5 μg of empty vector (-), FLAG-CDC25 (TOT), M1-FLAG-CDC25 (ER), LCK-FLAG-CDC25 (LR), CD8-FLAG-CDC25 (DM) and KDEL-FLAG-CDC25 (GC) where indicated. After 24 hours cells were serum deprived for 16 hours and lysed. Active Ras was pulled down using Raf-RBD. The figures are representative of 3 independent experiments.

Figure 3. Biochemical characterisation of Ras effector pathways activation. A. *ERK phosphorylation pattern is similar by comparing HRasV12 expression and HRas activation by CDC25*. NIH 3T3 cells were co-transfected in parallel with targeted FLAG-HRasV12 or targeted FLAG-CDC25 (0.5 μg) to different subcellular sites, M1 for ER, LCK for LR, CD8 for DM and KDEL for GC. Cells were serum deprived for 16 hours and the lysates were analysed by western blot by using specific antibodies. The blots were quantified using ImageJ and the graph shows average ERK phosphorylation normalised with respect to total ERK and relative to the negative control (empty vector) error bars show SD; n=3. B. *Ras activation from different localisation results on distinct level of Ras targets phosphorylation.* NIH 3T3 cells were transfected with 0.5 μg of empty vector, FLAG-CDC25 (TOT), M1-FLAG-CDC25 (ER), LCK-FLAG-CDC25 (LR), CD8-FLAG-CDC25 (DM) and KDEL-FLAG-CDC25 (GC). 24 hours post-transfection, the cells were starved for 7 hours and then lysed. Phosphorylation of the indicated proteins was determined by blotting with the indicated phospho-specific antibodies Corresponding total protein antibodies (anti-AKT, anti-JNK1 and anti-STAT3) were used for the normalisation of the data. The blots were quantified using ImageJ and the numbers show fold of phosphorylation normalised to the control (-); n=3.

Figure 4. Biological characterisation of Ras activation. A. *Compartmentalised CDC25 expression has an effect on cellular proliferation*. NIH 3T3 cells were seeded (50,000 cells/well) in six-well plate and transfected with 0.5 μg of the indicated CDC25 constructs. The proliferation rate of transfected cells, growing in media supplemented with 5% FBS, was monitored counting cells every 24 hours during 3 days. Data shows the average of three

independent experiments, error bars show SD. B. *Site-specific CDC25 do not confer bulk survival capacity*. Cells were seeded at high confluence (200,000 cells/well) in six-well plates and transfected with 0.5 μg of the indicated CDC25 constructs. Survival curves were monitored by counting cells every 24 hours for 3 days. Data shows the average of three independent experiments, error bars show SD C. *Colonies formation capacity is decreased by expression of targeted CDC25 in the endoplasmic reticulum*. NIH 3T3 were transfected with FLAG-CDC25, M1-FLAG-CDC25, LCK-FLAG-CDC25, CD8-FLAG-CDC25 or KDEL-FLAG-CDC25 (0.5 μg/plate). Transfected cells were selected in the presence of G418 (750 μg/ml). After 12-14 days in culture, colonies were Giemsa stained, and colonies with a diameter bigger than 0.5 mm were scored. Data shows the survival as the average of number of colonies ± SD of two independent experiments.

Figure 5. Physiological activation of Ras by CDC25. *Analysis of the transforming capacities of the CDC25 proteins.* NIH 3T3 cells were seeded in low density and transfected with 0.5 μg/plate pCEFL-FLAG, FLAG-CDC25 (TOT), M1-FLAG-CDC25 (ER), LCK-FLAG-CDC25 (LR), CD8-FLAG-CDC25 DM), KDEL-FLAG-CDC25 (GC) or 0.25 μg of FLAG-HRasV12. Transfected cells with HRasV12 (100 ng/plate) were used as positive control of foci formation. Foci were stained and scored after 3 weeks in culture. Images show pCEFL-FLAG and TOT-CDC25 cells stained at the indicated times. Numbers indicate average number of foci per μg of DNA ± SD of three independent experiments.

Figure 6. Summary of Ras effector pathway activation, and changes in phenotype mediated by endogenous HRas from different subcellular localisation. The scheme represents the HRas location specific activation effects observed in the current study. Font letter size indicates stronger effect.

Figure 1.

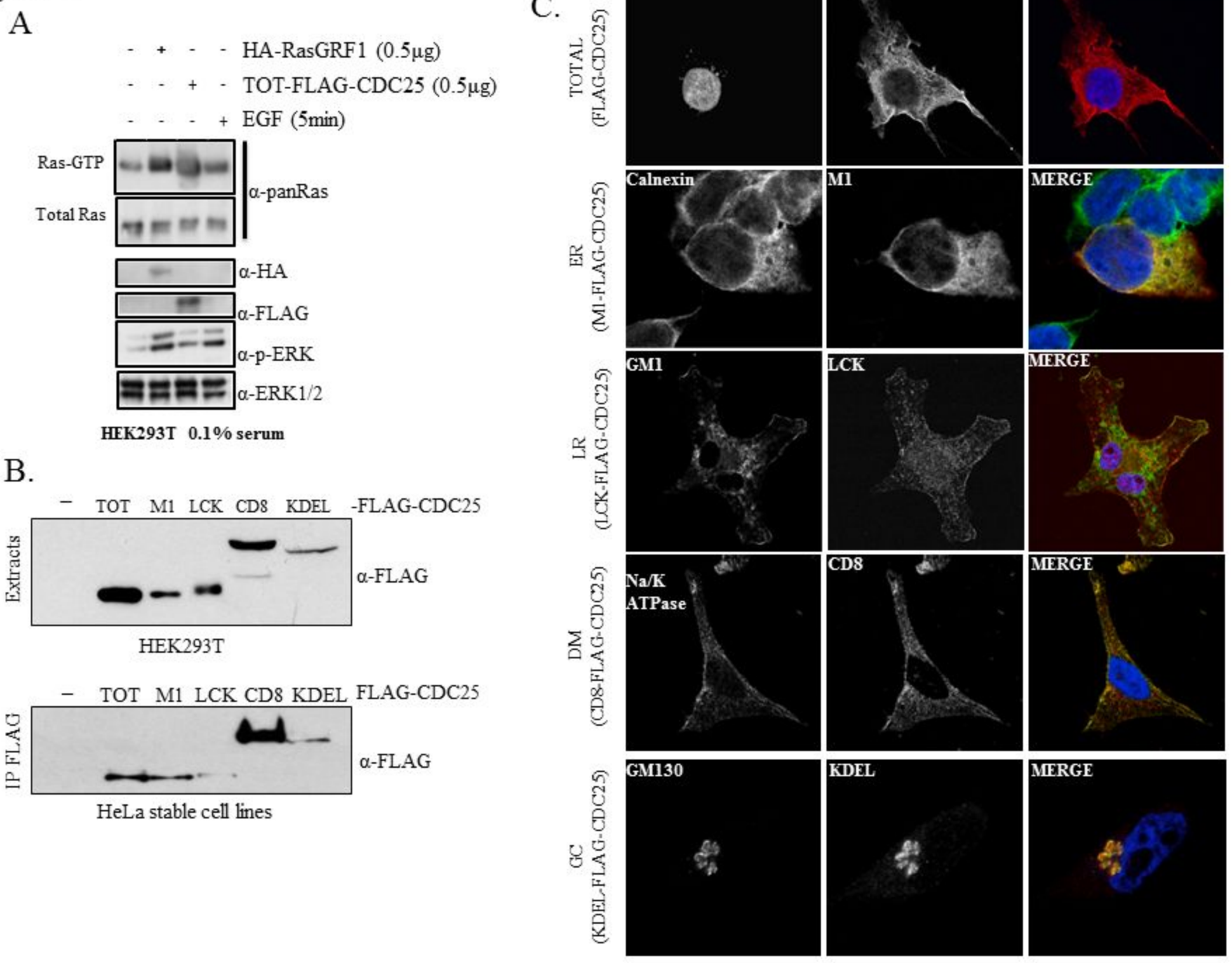
A
- + - - HA-RasGRF1 (0.5μg)
- - + - TOT-FLAG-CDC25 (0.5μg)
- - - + EGF (5min)
Ras-GTP
Total Ras
α-panRas
α-HA
α-FLAG
α-p-ERK
α-ERK1/2
HEK293T 0.1% serum
B.
– TOT M1 LCK CD8 KDEL -FLAG-CDC25
Extracts
α-FLAG
HEK293T
– TOT M1 LCK CD8 KDEL FLAG-CDC25
IP FLAG
α-FLAG
HeLa stable cell lines
C.
TOTAL (FLAG-CDC25)
DAPI
TOT
MERGE
ER (M1-FLAG-CDC25)
Calnexin
M1
MERGE
LR (LCK-FLAG-CDC25)
GM1
LCK
MERGE
DM (CD8-FLAG-CDC25)
Na/K ATPase
CD8
MERGE
GC (KDEL-FLAG-CDC25)
GM130
KDEL
MERGE

Figure 2.

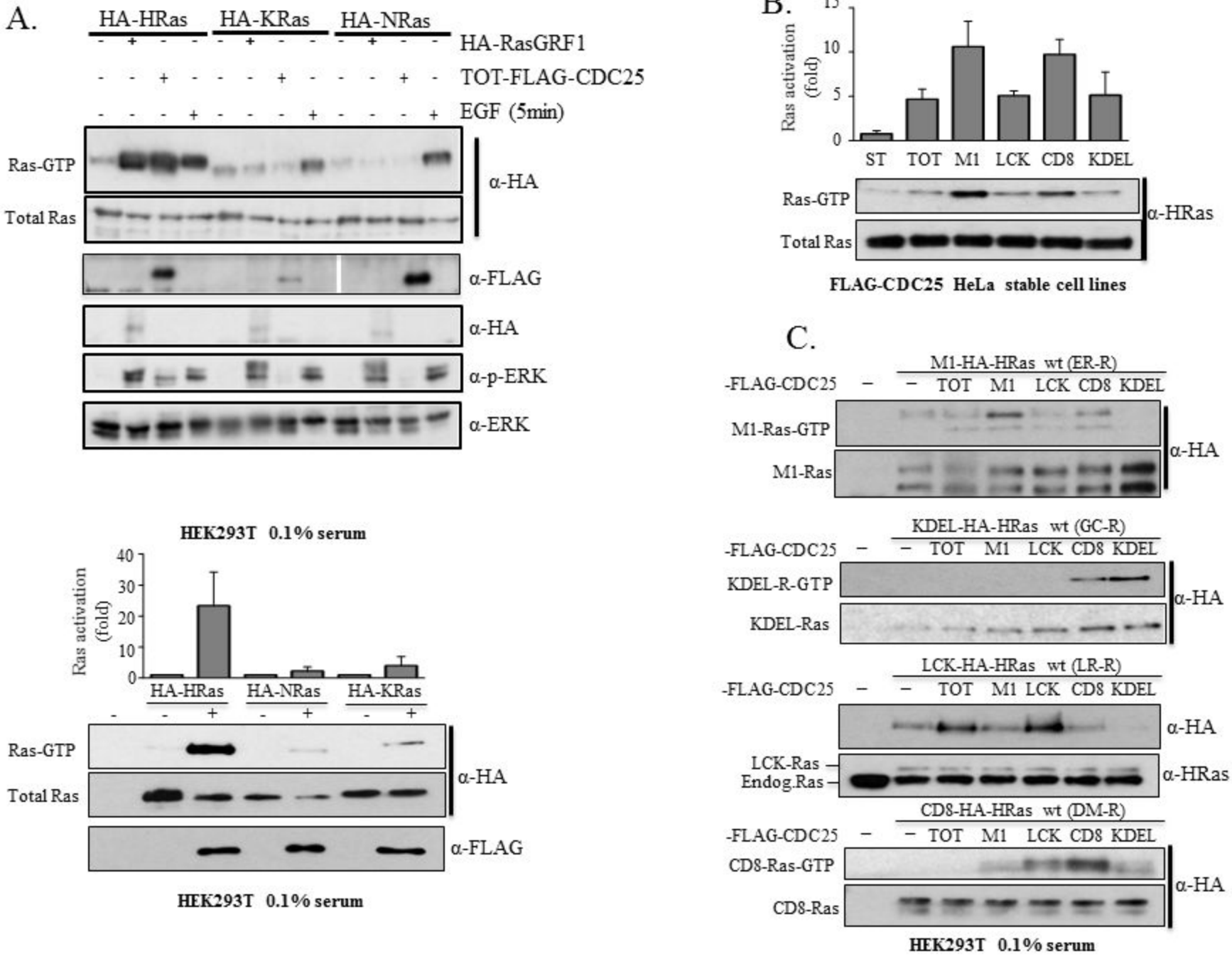
A.
HA-HRas
HA-KRas
HA-NRas
HA-RasGRF1
TOT-FLAG-CDC25
EGF (5min)
Ras-GTP
Total Ras
α-HA
α-FLAG
α-HA
α-p-ERK
α-ERK
HEK293T 0.1% serum
Ras activation (fold)
HA-HRas
HA-NRas
HA-KRas
Ras-GTP
Total Ras
α-HA
α-FLAG
HEK293T 0.1% serum
B.
Ras activation (fold)
ST
TOT
M1
LCK
CD8
KDEL
Ras-GTP
Total Ras
α-HRas
FLAG-CDC25 HeLa stable cell lines
C.
M1-HA-HRas wt (ER-R)
-FLAG-CDC25
TOT
M1
LCK
CD8
KDEL
M1-Ras-GTP
M1-Ras
α-HA
KDEL-HA-HRas wt (GC-R)
KDEL-R-GTP
KDEL-Ras
LCK-HA-HRas wt (LR-R)
LCK-Ras
Endog.Ras
CD8-HA-HRas wt (DM-R)
CD8-Ras-GTP
CD8-Ras
HEK293T 0.1% serum

Figure 3.

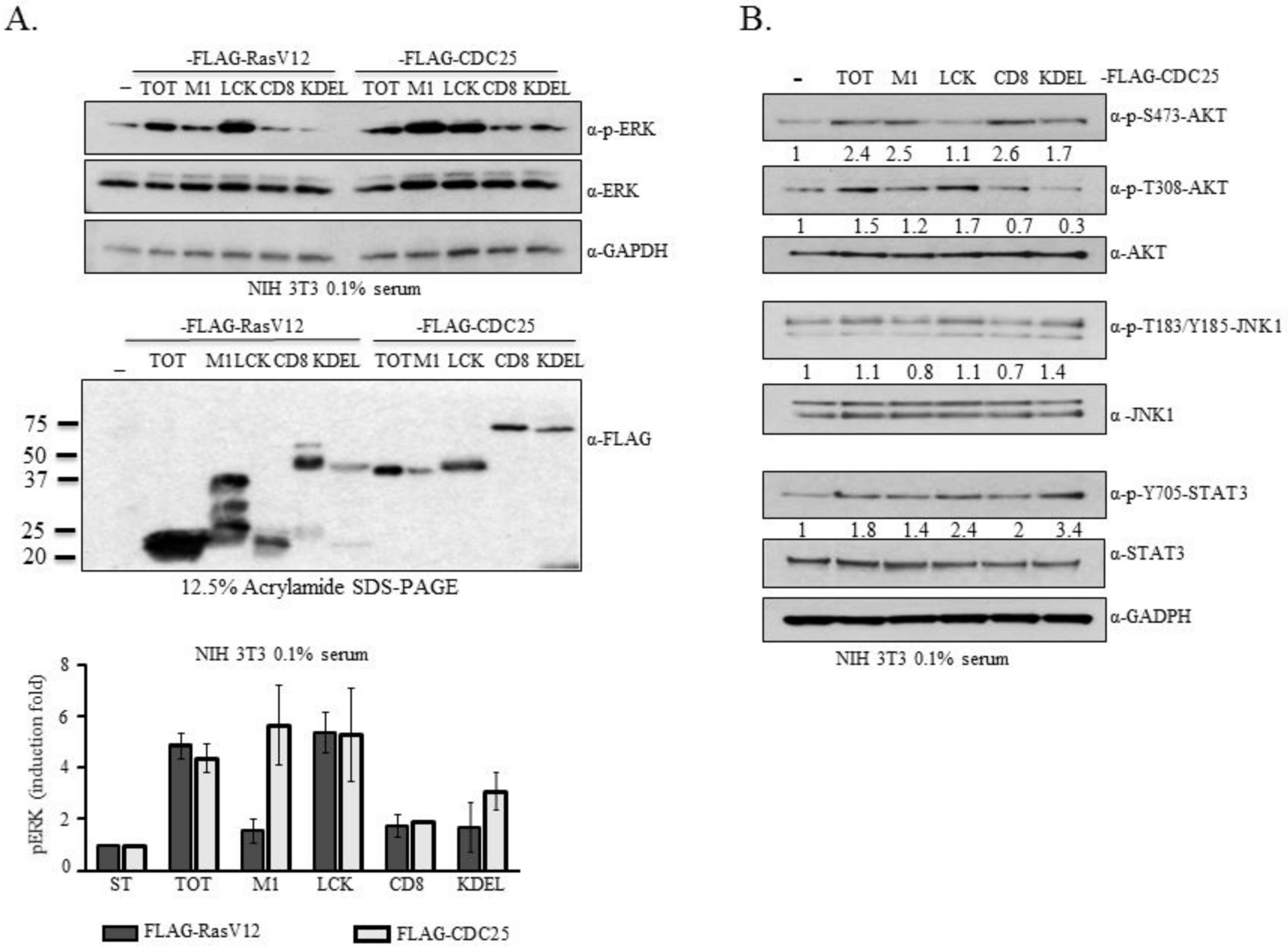
A.
-FLAG-RasV12
-FLAG-CDC25
– TOT M1 LCK CD8 KDEL TOT M1 LCK CD8 KDEL
α-p-ERK
α-ERK
α-GAPDH
NIH 3T3 0.1% serum
-FLAG-RasV12
-FLAG-CDC25
– TOT M1 LCK CD8 KDEL TOT M1 LCK CD8 KDEL
75
50
37
25
20
α-FLAG
12.5% Acrylamide SDS-PAGE
NIH 3T3 0.1% serum
pERK (induction fold)
8
6
4
2
0
ST TOT M1 LCK CD8 KDEL
FLAG-RasV12
FLAG-CDC25
B.
– TOT M1 LCK CD8 KDEL -FLAG-CDC25
α-p-S473-AKT
1 2.4 2.5 1.1 2.6 1.7
α-p-T308-AKT
1 1.5 1.2 1.7 0.7 0.3
α-AKT
α-p-T183/Y185-JNK1
1 1.1 0.8 1.1 0.7 1.4
α -JNK1
α-p-Y705-STAT3
1 1.8 1.4 2.4 2 3.4
α-STAT3
α-GADPH
NIH 3T3 0.1% serum

Figure 4

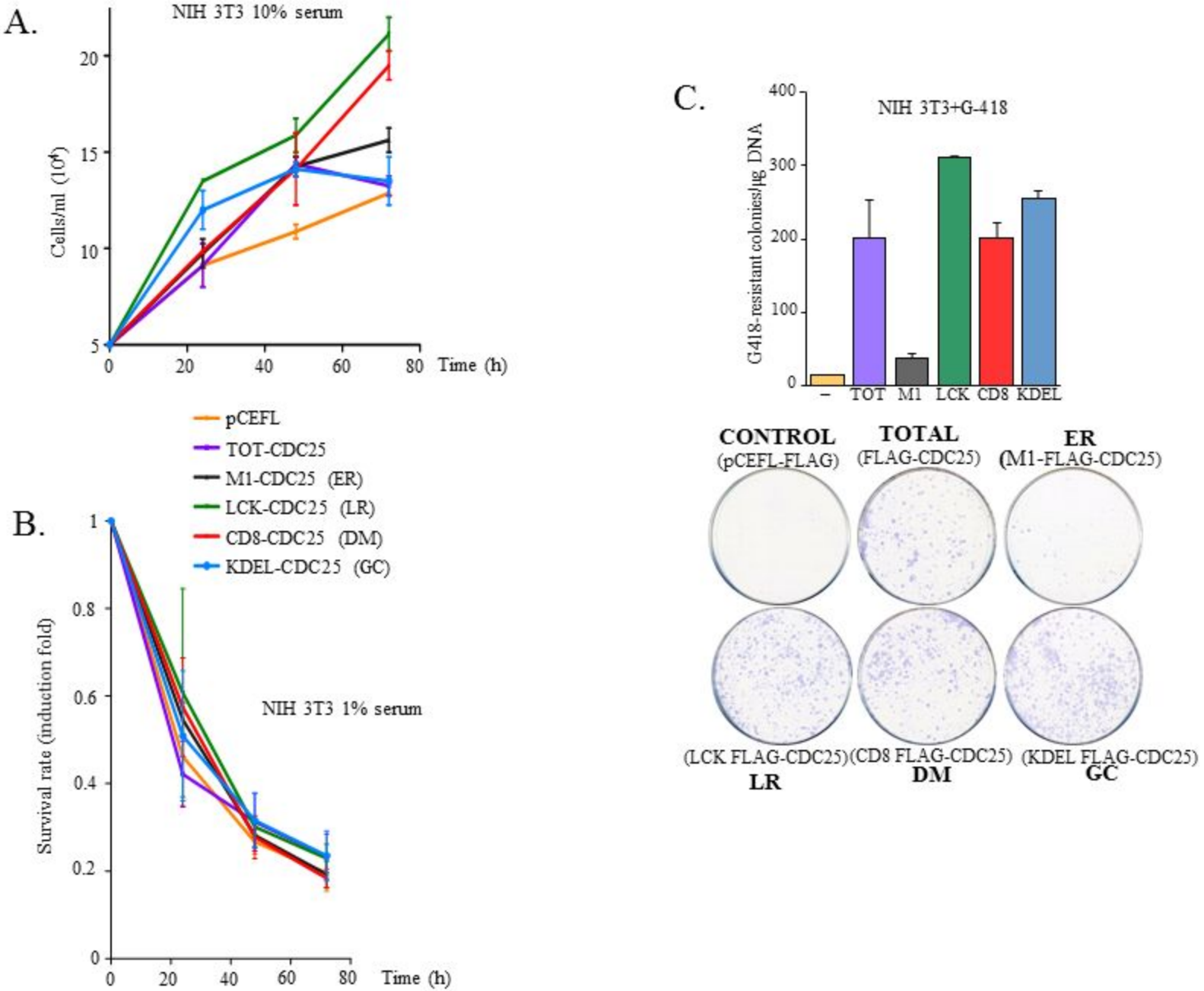
A.
NIH 3T3 10% serum
Cells/ml (10^4)
Time (h)
pCEFL
TOT-CDC25
M1-CDC25 (ER)
LCK-CDC25 (LR)
CD8-CDC25 (DM)
KDEL-CDC25 (GC)
B.
Survival rate (induction fold)
NIH 3T3 1% serum
Time (h)
C.
NIH 3T3+G-418
G418-resistant colonies/μg DNA
– TOT M1 LCK CD8 KDEL
CONTROL (pCEFL-FLAG)
TOTAL (FLAG-CDC25)
ER (M1-FLAG-CDC25)
(LCK FLAG-CDC25) LR
(CD8 FLAG-CDC25) DM
(KDEL FLAG-CDC25) GC

Figure 5

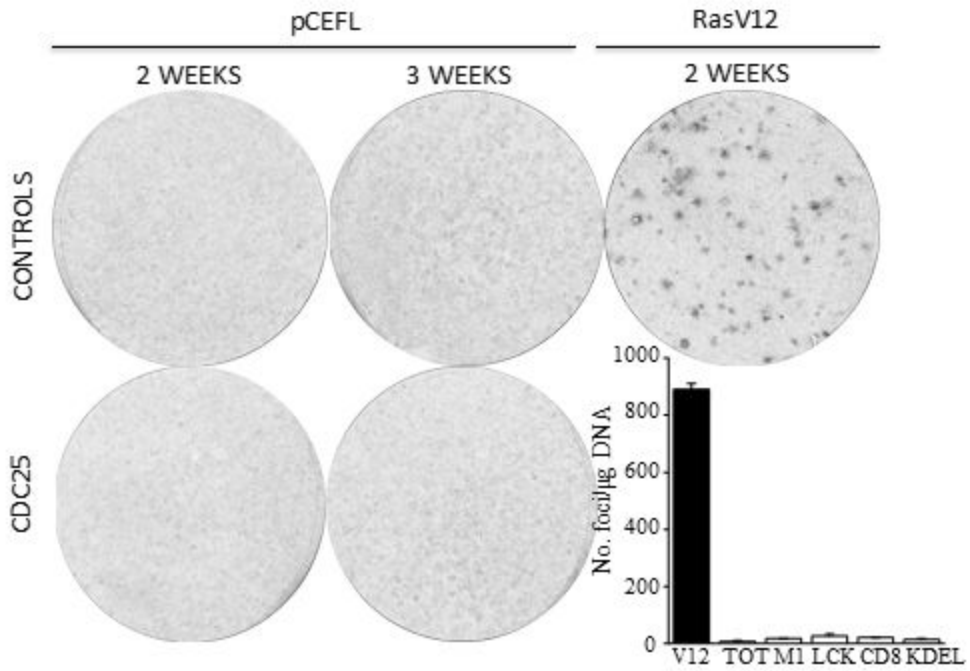
pCEFL
RasV12
2 WEEKS
3 WEEKS
2 WEEKS
CONTROLS
CDC25
No. foci/µg DNA
1000
800
600
400
200
0
V12
TOT
M1
LCK
CD8
KDEL

Figure 6

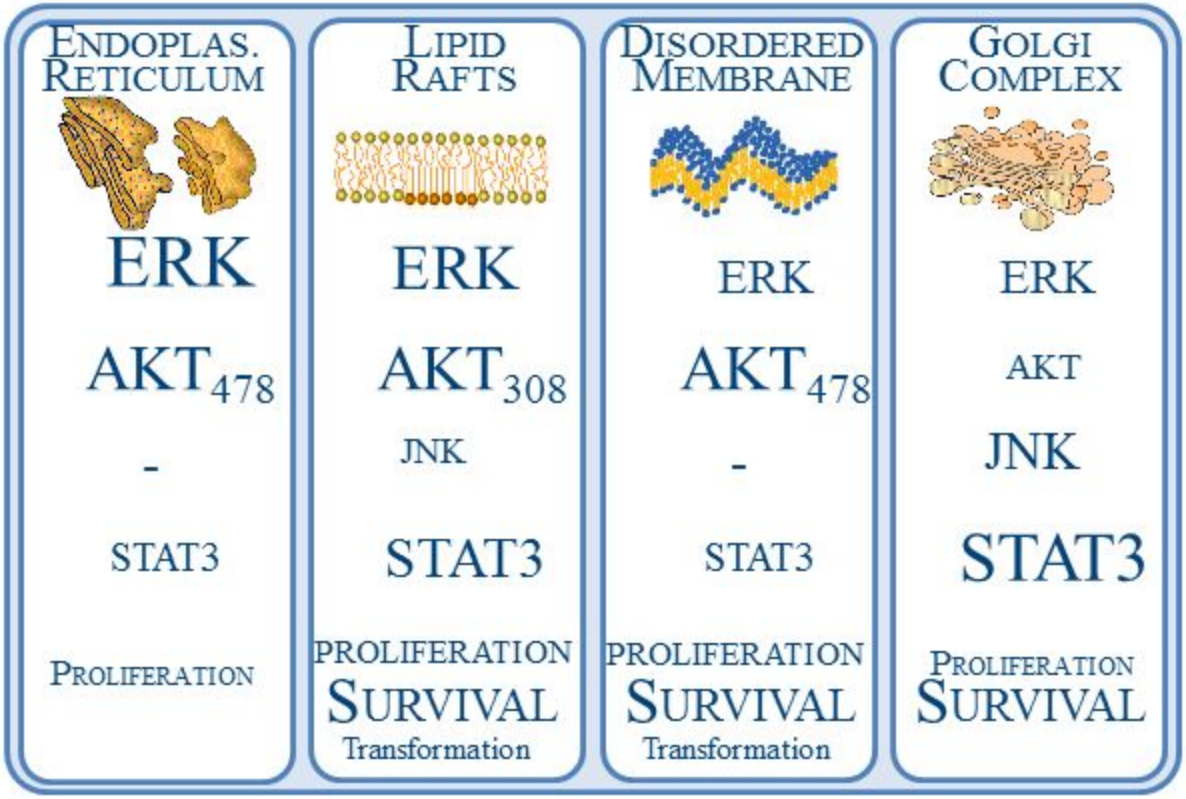
ENDOPLAS. RETICULUM
ERK
AKT478
-
STAT3
PROLIFERATION
LIPID RAFTS
ERK
AKT308
JNK
STAT3
PROLIFERATION
SURVIVAL
Transformation
DISORDERED MEMBRANE
ERK
AKT478
-
STAT3
PROLIFERATION
SURVIVAL
Transformation
GOLGI COMPLEX
ERK
AKT
JNK
STAT3
PROLIFERATION
SURVIVAL